Effect of crosslink torsional stiffness on elastic behavior of semiflexible polymer networks

H. Hatami-Marbini

Phys. Rev. E **97**, 022504 — Published 20 February 2018

DOI: 10.1103/PhysRevE.97.022504

Effect of Crosslink Torsional Stiffness on Elastic Behavior of Semiflexible Polymer Networks

H. Hatami-Marbini[1]

Department of Mechanical & Industrial Engineering, University of Illinois at Chicago, Chicago, IL 60607

[1] Email: hatami@uic.edu

Abstract

Networks of semiflexible filaments are building blocks of different biological and structural materials such as cytoskeleton and extracellular matrix. The mechanical response of these systems when subjected to an applied strain at zero temperature is often investigated numerically using networks composed of filaments, which are either rigidly welded or pinned together at their crosslinks. In the latter, filaments during deformation are free to rotate about their crosslinks while the relative angles between filaments remain constant in the former. The behavior of crosslinks in actual semiflexible networks is different than these idealized models and there exists only partial constraint on torques at crosslinks. The present work develops a numerical model in which two intersecting filaments are connected to each other by torsional springs with arbitrary stiffness. We show that fiber networks composed of rigid and freely rotating crosslinks are the limiting case of the present model. Furthermore, we characterize the effects of stiffness of crosslinks on effective elastic modulus of semiflexible networks as a function of filament flexibility and crosslink density. The effective elastic modulus is determined as a function of the mechanical properties of crosslinks and is found to vanish for networks composed of very weak torsional springs. Independent of the stiffness of crosslinks, it is found that the effective elastic modulus is a function of fiber flexibility and crosslink density. In low density networks, filaments primarily bend and the effective elastic modulus is much lower than the affine estimate. With increasing filament bending stiffness and/or crosslink density, the mechanical behavior of the networks becomes more affine and the stretching of filaments depicts itself as the dominant mode of deformation. The torsional stiffness of the crosslinks significantly affects the effective elastic modulus of the semiflexible random fiber networks.

Keywords: Elasticity, mechanical behavior, semiflexible polymer networks, crosslink stiffness

1. Introduction:

Semiflexible networks are composed of filaments that are crosslinked on the length scale of their thermal persistence length [1-4]. In these systems, the bending stiffness of the filaments cannot be ignored in comparison with their axial stiffness. In other words, the constituent filaments store strain energy in both bending and axial modes of deformation. Because of this property, the behavior of semiflexible networks, such as cytoskeleton of cells and extracellular matrix of tissues, is different than the behavior of flexible polymer networks.

There exists large literature on mechanical behavior of flexible fiber networks [5]. Classical rubber elasticity theory is often used to model the response of these polymeric networks. In this theory, it is assumed that filaments behave as Hookean springs and they store elastic energy because of the change in their end-to-end distance. Thus, flexible fibers are always in stretching and their deformation has no bending energy cost. Furthermore, the deformation field is assumed to be affine, i.e. the stretch and orientation of individual filaments can directly be obtained from the applied uniform far-field strain. The affine deformation assumption breaks down in semiflexible fiber networks because their constituent fibers store elastic energy by both bending and stretching. F-actin, DNA, collagen networks and carbon nanotubes are examples of semiflexible filaments [6-9]. The behavior of networks of semiflexible fibers cannot be accurately predicted using traditional flexible network theories [1-4].

In this work, we focus on the mechanical response of semiflexible filament networks at zero temperature. These networks are usually represented by Mikado Networks in computational studies, i.e. the network microstructure is created by random deposition of straight lines in a

square domain [10-14]. Although the nature of crosslinks is expected to have significant effects on the mechanical response, the intersecting lines in previous studies are modelled as either welded (rigid) or freely rotating crosslinks. Both crosslink types cause the translation of crossing filaments at their crosslink point to be the same. However, the latter allows free rotation, i.e. no constraint is applied on the continuity of bending moments at crosslinks. Wilhelm and Frey used Mikado model with both crosslink types to investigate the elasticity of random fiber networks [10]. They concluded that networks with rigid and freely rotating crosslinks behave similarly. They also found a scaling regime for which the behavior of these networks is bending dominated. Similar observation has been made by Head et al. using networks with freely rotating crosslinks [11]. They introduced a scalar quantity which can be used to determine whether the behavior of networks is affine or nonaffine. Hatami-Marbini and Picu characterized the effects of network microstructure and mechanical properties of filaments on nonaffine behavior of semiflexible fiber network using a strain-based nonaffinity measure [12,15]. In their study, they considered rigid crosslinks. Shahsavari and Picu showed that the relation between network effective elastic modulus and fiber density remains the same if welded or freely rotating crosslinks are used in numerical models [14]. In networks of semiflexible filaments such as carbon nanotubes, elasticity of crosslinks can be different than that of individual filaments [16-21]. For example, Terrones et al. showed that single-walled carbon nanotubes joined together by electron beam welding form stable junctions whose atomic arrangements are defective [21]. Thus, the mechanical behavior of junctions is expected to be different than the constituting carbon fibers and needs to be accounted for in the numerical simulations. Similarly, in systems such as F-actin fiber networks, the filaments are attached together via binding proteins whose elasticity defines the behavior of crosslinks and subsequently the whole fiber network [22,23].

For example, it has been observed that the elastic modulus of F-actin networks with the highly compliant filamin is much lower than that of rigidly crosslinked actin networks. However, despite their low elastic modulus, they could stiffen significantly and withstand large stresses [24,25]. These experimental observations have been described numerically by an effective medium theory and a numerical filamentous network model with compliant crosslinks [23,26,27]. In these previous studies, filaments are assumed to be infinitely rigid and their bending/stretching flexibility is neglected. In the present study, we extend these previous studies and investigate the effects of crosslink stiffness on the mechanical behavior of networks composed of semiflexible filaments. To this end, we develop a numerical model in which two intersecting filaments are connected to each other by torsional springs of adjustable stiffness. Networks composed of rigid, pinned jointed, and freely rotating crosslinks are the limiting cases of this model. We use Mikado algorithm to generate 2D random fiber networks and represent the crosslinks as hinges with torsional springs. The torsional springs connect filament segments together and stabilize the networks. Using this numerical model, we investigate the effects of torsional stiffness of crosslinks/junctions on the overall mechanical behavior of networks with different characteristics when subjected to small deformation. We present the results for sparse/dense Mikado networks composed of stiff/soft filaments. We find that the effective elastic modulus of the semiflexible random fiber networks is significantly reduced with decreasing the torsional stiffness of the crosslinks. Furthermore, we observe that torsional stiffness of the crosslinks has important effects on the range of network parameters over which the effective elastic modulus shows a power-law variation.

2. Numerical Model

Two dimensional random fiber networks are generated by deposition of straight lines in a square box of size L. The straight lines are of equal length L_0 and their orientation is obtained from a uniform distribution over $(0, \pi]$. The distance between two intersection points on a filament is called a segment length and is denoted by l_c. The mean segment length l_c is proportional to the fiber density ρ, defined as the total length of lines per unit area of the square box. Most likely, two lines will only intersect at each crossing point; however, since free dangling ends are eliminated, the mean coordination number of the networks will be less than 4. Filaments are modelled as linear elastic materials with bending stiffness $\kappa = E_f I$ and stretching stiffness $\mu = E_f A$, where E_f is Young's modulus, A is cross-sectional area, and I is the second moment of inertia of the filaments. The relative importance of bending stiffness and stretching stiffness is represented by filament flexibility parameter $l_b^2 = \kappa / \mu$. The filaments become more flexible with decreasing l_b. Note that l_c, l_b, L_0, and L are independent length scales of the problem. Here, we keep the ratio of L / L_0 large and use the initial filament length L_0 to normalize all other length scales. Moreover, we represent the network density by crosslink density L_0 / l_c which can be shown, in the high density networks, is proportional to network fiber density ρ, i.e. $L_0 / l_c \sim \rho$ [11]. Crosslinks are defined at intersection points of filaments, Figure 1. These crosslinks are modelled as torsional springs with torsional stiffness K_s, which is proportional to the bending stiffness of the neighboring filament segments, i.e. $K_s = \alpha < \kappa / l_c^3 >$ where α is a constant. When $\alpha \to \infty$, crosslinks become rigid connections (i.e., no rotation is allowed). They behave as

hinges when $\alpha \to 0$. In literature, the above limiting cases are often referred to welded (rigid) crosslinks and pin-jointed crosslinks, respectively. In this work, we vary the spring constant α to determine the effects of crosslink rigidity on the mechanical response of semiflexible fiber networks. Three types of crosslinks will be investigated: 1- Rigid crosslinks: where filaments are rigidly connected to each other, 2- Freely rotating crosslinks: where the moments are transferred along the individual filaments but not from one to another, and 3- Freely rotating crosslinks with torsional springs: where filament segments are allowed to rotate independent of each other and depending on the torsional spring constant α, Figure 1.

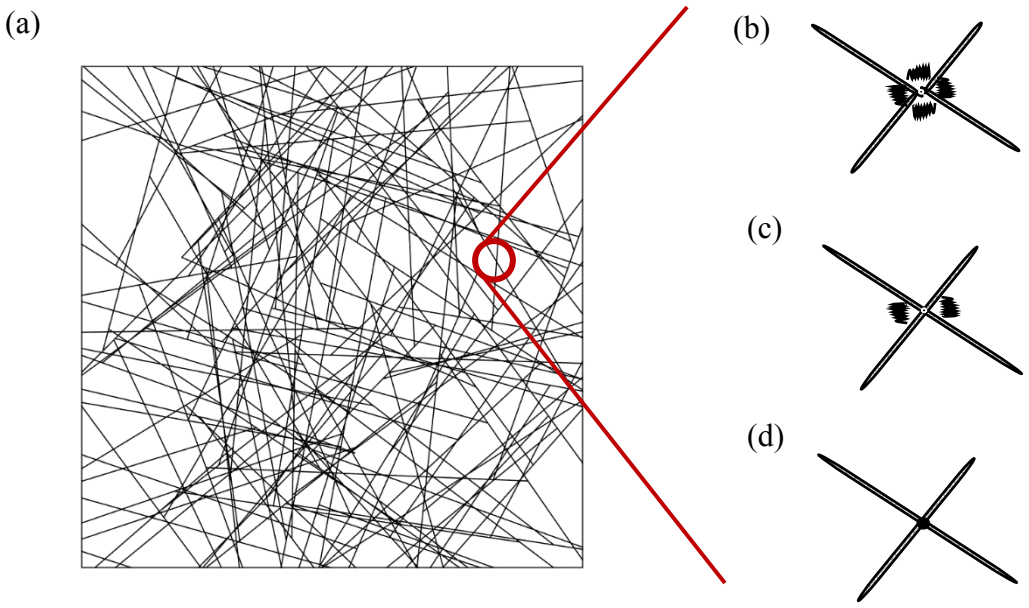

Figure 1. a) A typical random fiber network whose crosslinks are modelled as torsional springs with different spring constants. b) Four filament segments are pinned together at the crossing points and torsional springs resist the change of angle between them. c) Two filaments are pinned together at crossing point and torsional springs inhibit their free rotating. d) Two filaments are rigidly connected together at the crossing point.

The semiflexible fiber networks are subjected to uniaxial displacement boundary condition in x_1 direction. The corresponding strain field is $\varepsilon_{11} = \varepsilon_0$ and $\varepsilon_{12} = \varepsilon_{22} = 0$ where ε_0 is a nonzero small far-field strain. The total energy of the system at zero temperature is written as:

$$U = \frac{1}{2} \sum_{\text{fibers}} \int \left(\mu (u')^2 + \kappa (\phi')^2 \right) ds + \frac{1}{2} \sum_{\text{crosslinks}} K_s \psi^2 \qquad (1)$$

where ψ is the difference between current and reference angle at a crosslink, ϕ' is the curvature and u' is the axial strain along filaments whose contour length is parameterized by s. The elastic response of a single semiflexible polymer is not trivial and includes both energetic and entropic contributions. The system Hamiltonian, eq. (1), does not include the entropic contribution [10-12]. Nevertheless, it is still a popular model because it simplifies the numerical simulations while still capturing the anisotropic elastic response of filaments, i.e. the ratio of axial and bending stiffness is proportional to $(l_c / l_b)^2$ and significantly greater than 1 for typical system parameters. Note that when the temperature is nonzero, a semiflexible filament of length l_c with one end clamped has the transverse stiffness proportional to κ / l_c^3 and axial stiffness proportional to $\kappa^2 / (K_B T l_c^4)$ [10]. Thus, the ratio of axial and bending stiffness is proportional to $l_p / l_c > 1$, where l_p is the persistence length and is proportional to $\kappa / (K_B T)$. The readers are referred to other papers for the limitations of zero-frequency network models as well as recent advances on the semiflexible polymer elasticity at the molecular level [2,28-30].

The strain energy is computed numerically by discretizing the filament segments into several smaller segments and writing the discrete version of equation (1) in terms of degrees of freedom; more details can be found in references [11,12,31]. The solution for the degrees of freedom under the imposed uniaxial displacement boundary condition is obtained from minimizing the discrete form of the total energy using a finite element solver. In all simulations, we keep L / L_0 large in order to minimize finite size effects. The discrete form of equation (1) is then used to calculate the total energy U of the network when subjected to the uniform axial strain field $\varepsilon_{11} = \varepsilon_0$. The effective elastic modulus, E, of the semiflexible fiber network is obtained using $E \propto U / \varepsilon_0^2$ [11,31].

The affine effective elastic modulus E^{aff} can be obtained from the affine deformation assumption and by assuming that the mechanical response of network is only due to the stretching of the filaments. The axial deformation of a filament segment lying at an angle θ is $\varepsilon_0 l_c (1+\cos(2\theta)) / 2$ when the domain is subjected to far-field axial strain $\varepsilon_{11} = \varepsilon_0$. As stated in Section 2, the orientation of filaments in Mikado networks follows a uniform distribution function; thus, averaging the energy associated to all individual fiber segments gives $\frac{E^{affine}}{\mu} \propto \rho$ or $\frac{E^{affine} L_0}{\mu} \propto \frac{L_0}{l_c}$ when ρ is large.

In this work, we change the crosslink density from $L_0 / l_c \sim 10$ to 100, parameter l_b / L_0 from 10^{-7} to 10^{-1}, and torsional spring constant α from 10^{-15} to 10^{3} in order to investigate the effects of the torsional stiffness of crosslinks on the mechanical response of random semiflexible fiber networks. The results presented in this work are the averages over at least five replicas for each

case. Furthermore, since we did not perform any finite-size analysis, the results may involve some size effects [14,32].

3. Results and Discussion

Figure 2 plots the normalized effective Young's modulus as a function of torsional spring constant for filamentous networks with $L_0 / l_c = 30$ and $l_b / L_0 = 0.01$. It is seen that as the stiffness of the torsional springs at crosslinks reduces, there is a significant drop in the effective modulus. Moreover, this plot shows that the effective elastic modulus becomes negligible (and eventually vanishes) if the stiffness of torsional springs becomes much lower than the bending stiffness of the filaments. The effective elastic modulus reaches a plateau and becomes independent of the stiffness of the torsional springs when α become very large, i.e. the spring stiffness is significantly larger than the bending stiffness of filaments. In the limits $\alpha \to \infty$ and $\alpha \to 0$, the present numerical model captures the mechanical behavior of the semiflexible fiber networks with rigid and pin-jointed crosslinks, respectively.

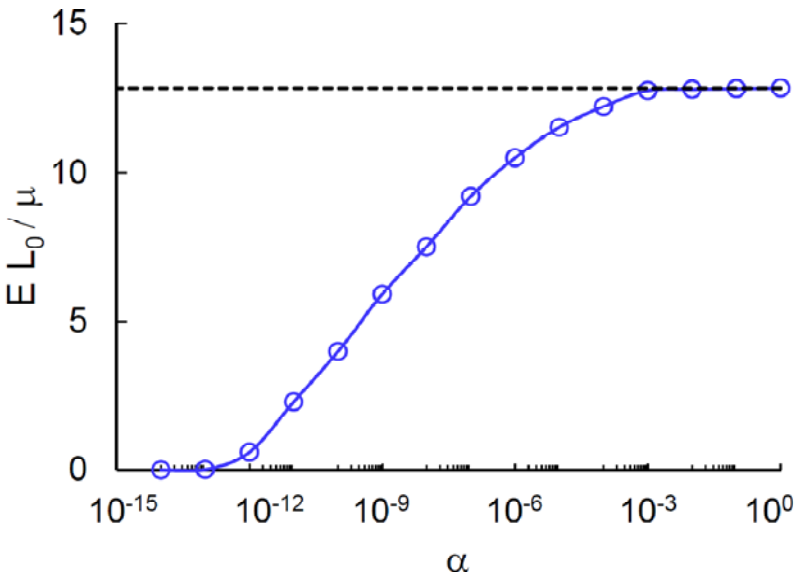

Figure 2. The normalized effective Young's modulus $E L_0 / \mu$ as a function of stiffness coefficient of torsional springs, α, for fiber networks with $L_0 / l_c = 30$ and $l_b / L_0 = 0.01$. In the limiting case of $\alpha > 10^{-3}$, crosslinks behave as rigid connections, the dashed line shows the results obtain from solution of fiber networks with rigid connection. When $10^{-15} < \alpha < 10^{-3}$, the effective stiffness of the network is decreasing with decreasing of α. The system becomes unstable and floppy for $\alpha < 10^{-15}$ due to numerical instabilities.

It has been shown that fiber networks created by Mikado algorithm reaches their geometric percolation when $L_0 / l_c \sim 5.4$ [11,33]. The geometric percolation occurs when there is at least one continuous path inside the domain. Nevertheless, this does not guarantee a nonzero stiffness for fiber networks. It has been shown that these networks reach their rigidity percolation at higher value of $L_0 / l_c \sim 5.9$ [10,11,34]. The rigidity percolation depends on the types of crosslinks and coordination number of the structure. The coordination number of a crossing point is defined as the number of line segments emerging from that point. Maxwell Counting Method states that two-dimensional pin-jointed frames will be rigid only if their coordination number is

greater than 4. In Mikado Networks, it is unlikely that more than two fibers cross at the same point. This means that the coordination number of most crosslinks is 4. However, Mikado generation algorithm yields a large number of dangling ends, which do not contribute to the total energy of the system under deformation. The removal of these dangling ends creates crosslinks with coordination number of 2 and 3, and subsequently, the mean coordination number becomes less than 4. Thus, Mikado networks are floppy if their crosslinks are pin-jointed, i.e. no bending moments are transferred (this is why the effective elastic modulus reduces to zero when $\alpha \to 0$ in Figure 2). In other words, without torsional springs, fiber networks accommodate the external deformation solely by rigid translation and rotation of their constituting filaments. Floppy pin-jointed Mikado networks can be made rigid by considering bending stiffness of the filaments and their bending at crosslinks, i.e. filaments should be able to resist bending modes of deformation and their independent rotations at the crosslinks should be prevented. In literature, this has been mainly done by assuming rigid crosslinks or freely rotating crosslinks. In both of these crosslink types, force and moment remain continuous along individual filaments; however, the angle of rotation is preserved along intersecting fibers in rigid crosslinks and changes from a fiber to another in freely rotating crosslinks. Freely rotating crosslinks are most commonly used in modelling actin filaments based on the assumption that binding proteins can only transfer forces between filaments. Nevertheless, it has been observed that using rigid crosslinks (which is computationally convenient) does not significantly affect the computational results especially if the fiber density is not close to the rigidity percolation.

Figure 2 shows that if α is large, the effective elastic modulus of the fiber networks becomes independent of the stiffness of torsional springs. In this limit, springs are much stiffer than the bending stiffness of neighboring filaments; therefore, crosslinks behave as if they are rigid

crosslinks. As stated in Section 2, mean segment length (l_c), filament flexibility parameter (l_b), and filament initial length (L_0) are independent length scales of the problem. Thus, the effective elastic modulus is a function of l_c, l_b, and L_0. Shahsavri and Picu calculated the effective elastic modulus of semiflexible fiber networks with welded (Fig. 1 c) and freely rotating (Fig. 1b) crosslinks [14]. Using the relation $\rho \sim 1 / l_c$ and by varying the exponents x and y in the expression $\log_{10} ((\rho L_0)^x / (l_b / L_0)^y)$, they were able to show that the effective elastic modulus collapses on a master curve if x = 7 and y = 2. In Figure 3, we compare the results of this work with this previous study. It is seen that the results of the present work, when the stiffness of torsional springs is large, match those obtained from modelling fiber networks with welded (rigid) crosslinks in Shahsavari and Picu. Moreover, we determined the effective elastic modulus of the fiber networks with freely rotating joints (Fig. 1b). For this purpose, we use stiff torsional springs ($\alpha \sim 10^3$) between segments of a filament at each crosslinks but soft torsional springs ($\alpha \sim 10^{-12}$) between segments of different filaments. We observed that the mechanical behavior of these networks was almost the same as the behavior of networks with rigid crosslinks (data not shown). Figure 3 shows that lowering the torsional stiffness of crosslinks results in a different behavior. Furthermore, a good collapse of data for these semiflexible networks is not observed. Thus, we conclude that the master curve given in Shahsavari and Picu's work depends on the behavior of crosslinks and cannot be used for all sparsely crosslinked fiber networks [14]. It remains for future studies to investigate the existence of such a mater curve for semiflexible fiber networks with compliant crosslinks. Despite this, Figure 3 shows that the normalized effective modulus approaches a horizontal asymptote as ρ and/or l_b become(s) very large. In this region, the effective elastic modulus has a linear scaling with density, as predicted by the affine deformation assumption.

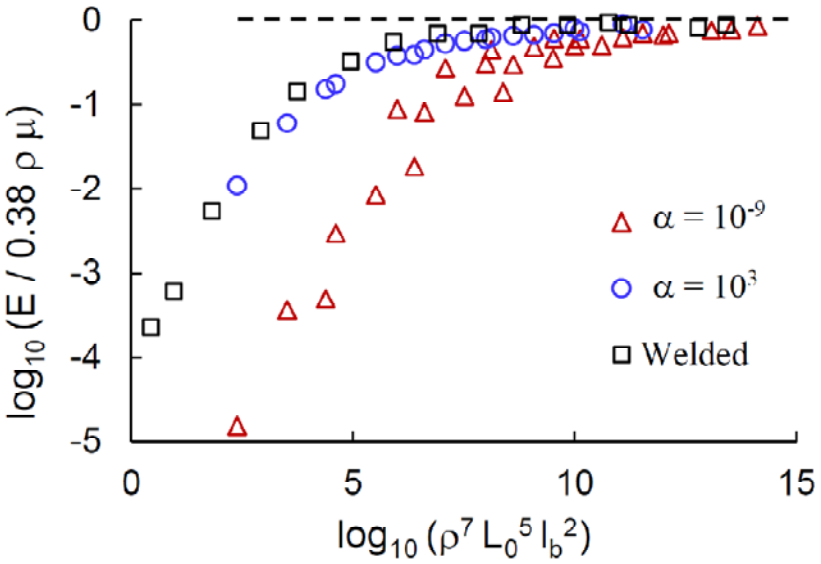

Figure 3. The normalized effective Young's modulus $\log_{10}(E / 0.38\,\rho\,\mu)$ for fiber networks with torsional springs with stiffness constant $\alpha = 10^{-9}$ (relatively soft crosslinks) and $\alpha = 10^{3}$ (relatively stiff crosslinks). The results for fiber networks with welded crosslinks from a previous study [15] is also shown for comparison. The data are for fiber networks with different crosslink density and filament flexibility parameter.

It is noted that, without torsional springs, fiber networks are floppy and accommodate the external deformation solely by rigid translation and rotation of their constituting filaments. In order to make these structures rigid, we should prevent free and independent rotations of filament segments at the crosslinks and assume that filaments resists bending modes of deformation as well as stretching ones. Figure 2 clearly captures this behavior and shows that the structures become floppy when the crosslinks start to behave as hinges. It is interesting to see whether the density of networks may have any influence on the behavior of these networks and

could possibly negate the effect of stiffness of crosslinks on the overall network rigidity. In Figure 4, we plot the effective Young's modulus as a function of crosslink density L_0 / l_c for networks with $l_b / L_0 = 10^{-4}$. We choose to plot $E L_0 / \mu$ because, as stated in section 2, $E^{affine} L_0 / \mu$ varies linearly with the crosslink density. A linear dependence of the Young's modulus with crosslink density is observed independent of the stiffness of torsional springs. The range of this linear dependence changes with stiffness of the torsional springs. Furthermore, for networks with similar fiber density, those with softer torsional springs have much lower effective elastic modulus. This figure suggests that decreasing the fiber density reduces the effective elastic modulus whether soft or stiff torsional springs are used at the crosslinks. In other words, fiber networks, independent of their number of density, become floppy when the stiffness of springs is significantly reduced. This is because the intrinsic randomness of the microstructure guarantees that filaments in these networks, independent of their density, deform rigidly when subjected to the far-field displacement. It is noted that this statement is only true for the response of these networks under small deformation (the scope of the present work). When subjected to finite deformation, the network microstructure is expected to align itself to the direction of the far-field load and resist further deformation.

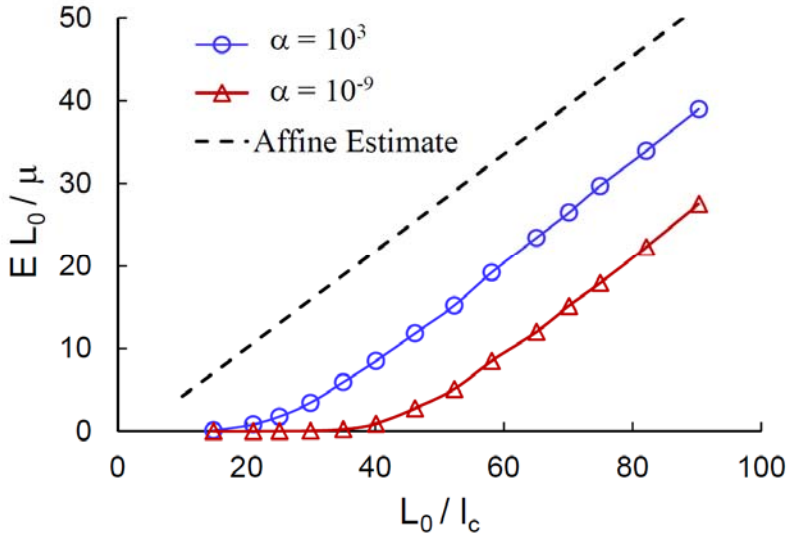

Figure 4. The normalized effective Young's modulus $E\,L_0 / \mu$ as a function of crosslink density L_0 / l_c for fiber networks with $\alpha = 10^3$ (rigid crosslinks) and $\alpha = 10^{-9}$ (relatively soft crosslinks) and $l_b / L_0 = 10^{-4}$. The dashed line shows the affine estimate of Young's modulus. It is seen that the torsional stiffness of the crosslinks significantly reduces the effective Young's independent of the crosslink density of the polymer network.

In addition to fiber density, the flexibility of the filaments should affect the response of fiber networks. The effect of stiffness of individual filaments is shown in Figure 5. As the stiffness of filaments decreases, the effective elastic modulus of the networks reduces following a power-law with power of 2, which means that $E \sim \kappa$. The same power-law relation is seen irrespective of the stiffness of the torsional springs when the constituting filaments become very soft. Nevertheless, the range of power-law behavior depends on the stiffness of springs: softer springs extend the range of this power-law dependence to larger l_b's. Outside the power-law relation, the normalized effective elastic modulus becomes independent of l_b, which means that $E \sim \mu$. When fibers are very flexible (very small l_b / L_0), the energy cost of bending deformation modes

becomes significantly less than the cost of their stretching ($\kappa << \mu$). Thus, the dominant mode of deformation is bending. However, as fibers become stiff, their stretching becomes energetically favorable. Thus, a transition in the behavior of the network is expected with increasing parameter l_b / L_0 and/or crosslink density L_0 / l_c.

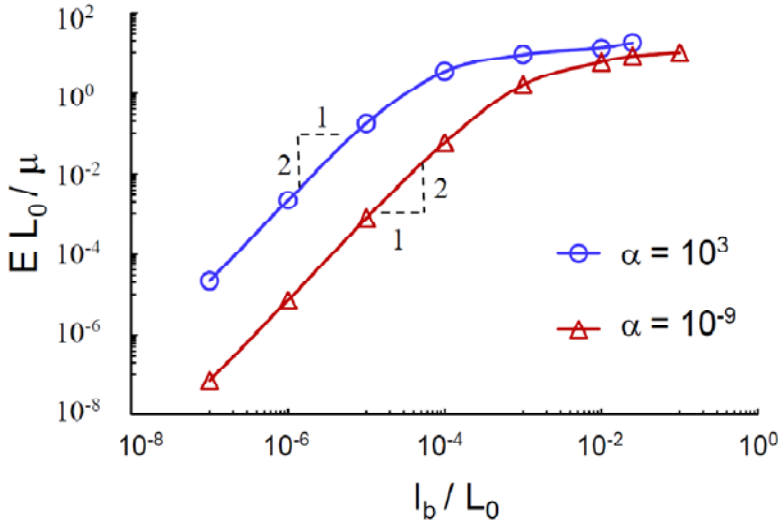

Figure 5. The normalized effective Young's modulus $E L_0 / \mu$ as a function of filament flexibility parameter l_b / L_0 for fiber networks with $\alpha = 10^3$ (relatively stiff crosslinks) and $\alpha = 10^{-9}$ (relatively soft crosslinks) and $L_0 / l_c = 30$. It is seen that the torsional stiffness of the crosslinks significantly reduces the effective Young's modulus independent of the flexibility of constituent filaments. Furthermore, a bending dominated region (lines with slope 2) exist independent of stiffness of torsional springs.

In Figure 6, we plot the ratio of axial energy U^{axial} and total strain energy U^{total} of fiber networks with crosslink density $L_0 / l_c \sim 30$. The data presented in this plot provides further support for the above discussion: U^{axial} / U^{total} increases with increasing l_b / L_0. This ratio is independent of the

stiffness of crosslinks when l_b / L_0 is less than a critical value. Nevertheless, as the filament rigidity increases, fiber networks with stiff crosslinks show a different response than those with softer crosslinks. This behavior is observed because, as discussed earlier, Mikado fiber networks with pinned crosslinks are floppy and their deformation includes rigid rotation of filaments at certain numbers of crosslinks. The soft torsional springs accommodate these rigid rotations without significant bending of filaments. Nevertheless, when these springs become stiff, they require the filaments to bend, no matter how energetically costly their bending is, in order to keep the whole structure rigid. Thus, the ratio U^{axial} / U^{total} is expected to decrease as it is captured in our numerical simulations, Figure 6. Because of this behavior, the effective elastic modulus of these networks will not converge to the prediction of the affine model. The affine estimate assumes that affine rotation of filaments does not incur any cost to the total energy of the system. Nevertheless, this assumption is not true for fiber networks composed of rigidly crosslinked filaments. For these networks, affine estimate should be obtained by accounting for the bending of filaments in addition to their stretching [35].

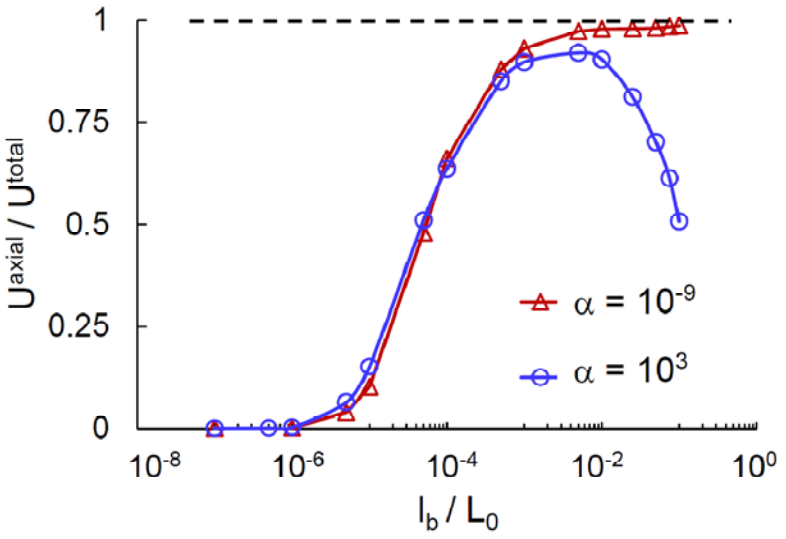

Figure 6. The ratio of axial energy and total strain energy as a function of filament flexibility parameter l_b / L_0 for fiber networks with $\alpha = 10^3$ (relatively stiff crosslinks) and $\alpha = 10^{-9}$ (relatively soft crosslinks) and crosslink density of $L_0 / l_c = 30$. With increasing rigidity of filaments, the behavior of the fiber networks becomes stretching dominant. Nevertheless, for networks with rigid crosslinks, there exist a critical l_b / L_0 greater than which the bending modes become important again. This critical value depends on crosslink density L_0 / l_c.

In conclusion, we develop a numerical model for the mechanical behavior of semiflexible fiber networks in which filaments are connected together by torsional springs with adjustable stiffness. This model is more general than previous numerical models in the literature and gives a more realistic representation of the behavior of semiflexible networks, such as carbon nanotubes, whose crosslinks cannot fully transfer moments between individual fiber segments. We find that the stiffness of crosslinks has a significant effect on the effective stiffness of the structure independent of other parameters defining the network elasticity. Moreover, it is found that the

effective elastic modulus of fiber networks with crosslinks of different stiffnesses has a relatively similar power law dependence on the filament flexibility parameter l_b. This power-law behavior exists when the dominant mode of deformation is bending and its range depends on the stiffness of torsional springs. The effect of crosslink density on the stiffness of the networks is also determined. Although the system becomes stiffer with increasing crosslink density, networks composed of soft crosslinks have a much lower elastic modulus compared to those with stiffer crosslinks. The present model can be extended in future studies such that it includes the axial elasticity of crosslinks in addition to their torsional stiffness. Furthermore, the findings of the present work are pertinent to the linear elastic response of the networks under small strain. Future studies are needed to determine the nonlinear behavior of networks subjected to large deformation when crosslinks are modelled as torsional springs.

Acknowledgement

The author gratefully acknowledges support for this work in part from NSF-CMMI-1351461.

References

[1] H. Hatami-Marbini and C. Picu, in *Advances in Soft Matter Mechanics*, edited by S. Li, and B. Sun (Springer Heidelberg, 2012), pp. 119.

[2] C. P. Broedersz and F. C. MacKintosh, Rev. Mod. Phys. **86**, 995 (2014).

[3] R. Picu, Soft Matter **7**, 6768 (2011).

[4] C. Storm, J. J. Pastore, F. C. MacKintosh, T. C. Lubensky, and P. A. Janmey, Nature **435**, 191 (2005).

[5] M. Rubinstein and R. H. Colby, *Polymer physics* (Oxford University Press New York, 2003), Vol. 23.

[6] F. Gittes, B. Mickey, J. Nettleton, and J. Howard, The Journal of Cell Biology **120**, 923 (1993).

[7] Z. Dogic *et al.*, Phys. Rev. Lett. **92**, 125503 (2004).

[8] N. Fakhri, D. A. Tsyboulski, L. Cognet, R. B. Weisman, and M. Pasquali, Proceedings of the National Academy of Sciences **106**, 14219 (2009).

[9] A. J. Licup, S. Münster, A. Sharma, M. Sheinman, L. M. Jawerth, B. Fabry, D. A. Weitz, and F. C. MacKintosh, Proceedings of the National Academy of Sciences **112**, 9573 (2015).

[10] J. Wilhelm and E. Frey, Phys. Rev. Lett. **91**, 108103 (2003).

[11] D. A. Head, A. J. Levine, and F. C. MacKintosh, Phys. Rev. E **68**, 061907 (2003).

[12] H. Hatami-Marbini and R. Picu, Phys. Rev. E **77**, 062103 (2008).

[13] P. Onck, T. Koeman, T. Van Dillen, and E. Van der Giessen, Phys. Rev. Lett. **95**, 178102 (2005).

[14] A. Shahsavari and R. Picu, Phys. Rev. E **86**, 011923 (2012).

[15] H. Hatami-Marbini and R. Picu, Acta Mech. **205**, 77 (2009).

[16] A. Saha, C. Jiang, and A. A. Martí, Carbon **79**, 1 (2014).

[17] Z. Lu, M. Zhu, and Q. Liu, J. Phys. D: Appl. Phys. **47**, 065310 (2014).

[18] B. Xie, Y. Liu, Y. Ding, Q. Zheng, and Z. Xu, Soft Matter **7**, 10039 (2011).

[19] S. Gong and Z. Zhu, Nanoscale **7**, 1339 (2015).

[20] S. W. Cranford and M. J. Buehler, Nanotechnology **21**, 265706 (2010).

[21] M. Terrones, F. Banhart, N. Grobert, J.-C. Charlier, H. Terrones, and P. Ajayan, Phys. Rev. Lett. **89**, 075505 (2002).

[22] B. Wagner, R. Tharmann, I. Haase, M. Fischer, and A. R. Bausch, Proceedings of the National Academy of Sciences **103**, 13974 (2006).

[23] C. P. Broedersz, C. Storm, and F. C. MacKintosh, Phys. Rev. Lett. **101**, 118103 (2008).

[24] M. L. Gardel, F. Nakamura, J. Hartwig, J. C. Crocker, T. P. Stossel, and D. A. Weitz, Phys Rev Lett **96**, 088102 (2006).

[25] M. L. Gardel, F. Nakamura, J. H. Hartwig, J. C. Crocker, T. P. Stossel, and D. A. Weitz, Proceedings of the National Academy of Sciences of the United States of America **103**, 1762 (2006).

[26] A. Sharma, M. Sheinman, K. Heidemann, and F. MacKintosh, Phys. Rev. E **88**, 052705 (2013).

[27] K. M. Heidemann, A. Sharma, F. Rehfeldt, C. F. Schmidt, and M. Wardetzky, Soft Matter **11**, 343 (2015).

[28] J. F. Marko and E. D. Siggia, Macromolecules **28**, 8759 (1995).

[29] E. Frey, K. Kroy, J. Wilhelm, and E. Sackmann, in *Dynamical Networks in Physics and Biology* (Springer, 1998), pp. 103.

[30] A. Dhar and D. Chaudhuri, Phys. Rev. Lett. **89**, 065502 (2002).

[31] H. Hatami-Marbini and R. C. Picu, Phys. Rev. E **80**, 046703 (2009).

[32] A. Shahsavari and R. Picu, International Journal of Solids and Structures **50**, 3332 (2013).

[33] G. Pike and C. Seager, Phys. Rev. B **10**, 1421 (1974).

[34] M. Latva-Kokko and J. Timonen, Phys. Rev. E **64**, 066117 (2001).

[35] X.-F. Wu and Y. A. Dzenis, J. Appl. Phys. **98**, 093501 (2005).